NSR-33-009-029

1967 HEAT TRANSFER AND FLUID MECHANICS INSTITUTE

FACILITY FORM 602
N68-27527 (ACCESSION NUMBER) (THRU) 1
35 (PAGES) (CODE)
CR-82455 (NASA CR OR TMX OR AD NUMBER) 12 (CATEGORY)

HYPERSONIC TURBULENT BOUNDARY LAYER STUDIES AT COLD WALL CONDITIONS

GPO PRICE $ _____

CFSTI PRICE(S) $ _____

Hard copy (HC) _____

Microfiche (MF) _____

ff 653 July 65

by

J.E. WALLACE

FEBRUARY 1967



AERODYNAMIC RESEARCH DEPARTMENT
CORNELL AERONAUTICAL LABORATORY, INC.
BUFFALO, NEW YORK 14221

HYPERSONIC TURBULENT BOUNDARY LAYER STUDIES AT COLD WALL CONDITIONS

by

J.E. Wallace*

Aerodynamic Research Department
Cornell Aeronautical Laboratory, Inc.
Buffalo, New York 14221

ABSTRACT

In this paper the results of a series of shock tunnel experiments on hypersonic turbulent-boundary-layer flow over flat plates with sharp and blunt leading edges and on the wall of a contoured expansion nozzle are presented. The ratio of wall temperature to stagnation temperature ranged from 0.14 to 0.3 on the flat plate and from 0.09 to 0.3 on the nozzle wall. Simultaneous measurements of skin friction and heat transfer were obtained. Comparison of the experimental skin friction results with those obtained using semi-empirical compressible turbulent boundary layer methods indicates best agreement with the method of Spalding and Chi. The experimental heat transfer measurements indicate that under these cold wall conditions the ratio of heat transfer rate to skin friction is smaller than is predicted by current theory. The experimental data are also used to determine corrections to the Crocco relation between the velocity and total enthalpy profiles. These corrections are found to be consistent with direct measurements of total temperature profiles by other investigators. A tentative equivalence is found between the measurements on the sharp flat plate and those on the wall of the contoured nozzle.

*Associate Aeronautical Engineer.

INTRODUCTION

Knowledge of highly cooled turbulent boundary layers at hypersonic Mach numbers is important in the aerodynamic and thermodynamic design of a whole family of hypersonic vehicles of current interest. The fundamental complexity of turbulent flows and the accompanying difficulty of theoretical description -- even for incompressible turbulent flows -- has led, in the case of compressible turbulent flows, to numerous attempts to relate the compressible case to the incompressible one, for which a considerable body of experimental data exists. Approaches which have been proposed are: 1) transformations of the compressible flow to a corresponding incompressible one, for example, Cohen (Ref. 1) and the work of Coles (Ref. 2) extended by Crocco (Ref. 3) and applied by Baronti and Libby (Ref. 4), 2) reference temperature (or enthalpy) methods, for example, Monaghan (Ref. 5) and Eckert (Ref. 6), and 3) other semi-empirical methods, such as that of Spalding and Chi (Ref. 7). The nozzle design calculation methods suggested by Bartz (Ref. 8) for rocket nozzles and Wood (Ref. 9) for hypersonic wind tunnel nozzles rely upon reference temperature applications of adiabatic wall, zero-pressure-gradient-constant-density results. Hence, it is evident that knowledge of the shear law, the relationship between skin friction and heat transfer, and of the boundary layer profiles in compressible turbulent flow is required to guide the development and assess the validity of theory.

Recent compilations by Spalding and Chi (Ref. 7) and Bertram and Neal (Ref. 10) indicate current flat-plate turbulent-flow data are limited to reservoir temperatures below 1800°R and to ratios of wall temperature to stagnation temperature greater than 0.5. Thus, there is a lack of experimental data at conditions approximating those of hypersonic flight; i.e., simultaneously high Reynolds numbers, high total enthalpy and high heat transfer rates to the surface (cold walls) at high local Mach numbers. Furthermore, the analysis of existing experimental data on compressible turbulent flow is hampered by the absence of simultaneous, direct measurement of skin friction and heat transfer, except in the measurements reported

by Neal (Ref. 11). There,a single skin-friction panel on a flat plate was employed in flows with reservoir temperatures of 1100°R and a ratio of wall temperature to stagnation temperature of 0.5. Although attempts have been made to compute skin friction from boundary layer profile measurements, Rotta (Ref. 12) and Walz (Ref. 13) have shown that widely varying results can be calculated depending upon the approach and assumptions used.

In the experiments reported herein, skin friction was measured directly on flat plate models with sharp and blunt (cylindrical, two-inch diameter) leading edges and on a shock tunnel nozzle wall. The flat plate data provide a basis for comparison with theory using a simple, well-defined geometry and flow history. In the nozzle experiments pitot pressure measurements were obtained across the boundary layer thickness (two to four inches) and were used to compute a local momentum thickness for comparisons between the wall measurements and theory. Thus, the present work provides information for the evaluation and further development of methods for the analysis of hypersonic, highly cooled, turbulent boundary layers.

EXPERIMENTAL PROGRAM

Flat Plate

The investigations of turbulent boundary-layer flow over flat plates were conducted with air in the Cornell Aeronautical Laboratory 8-Foot Hypersonic Shock Tunnel using contoured expansion nozzles. Simultaneous measurements of skin friction, heat transfer rates, and static pressure on the flat plate surface were obtained at numerous points on the flat plate surface as shown in Figure 1. The direct skin friction measurements were made using a piezoelectric crystal transducer, whose development is described in Ref. 14. Temperature histories obtained with thin film (platinum) resistance, thermometers were converted directly to heat transfer rates using analog circuits described in Ref. 15.

The nominal test conditions were as follows:

Condition	Reservoir Temperature T_o (°R)	Reservoir Pressure P_o (psia)	Free-Stream Temperature T_∞(°R)	T_w/T_o	Mach Number	Reynolds Number (per ft)	Angle of Attack (degrees)
1	3800	19,000	355.2	0.14	7.4	20×10^6	0, 5, 10
2	1800	20,000	125	0.3	8.1	81×10^6	0, 5, 10
3	2800	18,500	125	0.19	10.7	12×10^6	0, 5, 10, 20
4	2400	4,500	210	0.22	7.4	9×10^6	0

Substantial lengths of fully developed turbulent flow were obtained at all conditions. On the sharp flat plate at zero-incidence the minimum turbulent flow length was 12 inches at the Mach number 10.7 condition, while for the Mach number 8.1 condition the boundary layer transition was completed at the first instrumented station, yielding nearly two feet of fully developed turbulent flow. Boundary layer transition was completed on the leading edge at Mach numbers of 7.4 and 8.1 for the blunt leading edge configuration, while downstream transition for the Mach number 10.7 tests produced at least 18 inches of turbulent flow. For the sake of brevity the flat-plate-heat transfer data have been used here only in comparison with the skin friction measurements. A more detailed description of the test apparatus and of the test data, including the heat transfer results, is provided in Ref. 16.

Nozzle Wall

The two-foot exit diameter, contoured, axisymmetric nozzle (nominal Mach number of 8) of the CAL Hypersonic Shock Tunnel was instrumented with pressure, heat transfer and skin friction gages at four stations along the last four feet (Figure 2). In addition, a pitot pressure rake which spanned the boundary layer thickness was positioned one inch downstream from the last station of surface instrumentation. In all cases the nozzle throat Reynolds numbers were well above those required for turbulent flow at the throat; thus turbulent flow was attained in the nozzle boundary layer. The measured wall pressures indicate that the relative axial pressure gradient at the nozzle exit, dp_e/dx, is less than 0.2 per foot.

Nominal test conditions were as follows:

Condition*	Reservoir Temperature T_o (°R)	Reservoir Pressure P_o (psia)	Free-Stream Temperature T_e (°R)	T_w/T_o	Exit Mach Number	Reynolds Number (per foot)
1**	1850	4200	140	.29	8.0	11×10^6
2	1800	1000	150	.30	7.8	2.6×10^6
3	5750	1000	740	.093	6.6	0.37×10^6
4	5000	930	590	.11	6.8	0.44×10^6
5***	2300	2300	190	.23	7.8	4.1×10^6
6	2400	5700	180	.22	8.0	9.7×10^6
7	2200	520	190	.24	7.6	1.0×10^6

* Repeat runs were made at each condition. Test gas was air in all cases.

** Runs 1-4: wall and profile measurements.

*** Runs 5-7: wall measurements only.

DISCUSSION OF RESULTS

Flat Plate Results

Since heavy reliance has been placed in the past upon the reference enthalpy method for extending the incompressible, zero-pressure gradient shear laws, this approach has been examined here. The Eckert reference enthalpy (Ref. 6)

$$h_{*_{Eckert}} = 0.5 H_w + 0.28 h_e + 0.22 H_{AW} \qquad (1)$$

has been used to evaluate the density and viscosity in the Blasius shear law (Ref. 17)

$$\frac{\tau}{\frac{1}{2}\rho_* u_e^2} = \frac{2A}{\left(\frac{\rho_* u_e x}{\mu_*}\right)^n} \qquad (2)$$

where for laminar flow $A = 0.332$, $n = 0.5$ and for turbulent flow $A = 0.0296$, $n = 0.2$. If this shear law is substituted in the flat plate, zero-pressure gradient momentum equation

$$\frac{d\theta}{dx} = \frac{\tau}{\rho_e u_e^2}$$

the integration for momentum thickness yields

$$\frac{\theta}{x} = \frac{A}{1-n} \frac{\rho_*}{\rho_e} \left(\frac{\rho_* u_e x}{\mu_*} \right)^{-n} \qquad (3)$$

An effective turbulent flow length, x', has been computed for each of the test cases by solving for the turbulent flow length required to produce a turbulent momentum thickness at transition equal to the computed laminar momentum thickness at the experimentally observed transition distance from the leading edge. The positions of the peak values observed in the heat transfer and skin friction data were used to locate the transition point.

The zero angle of attack data at the Mach number 7.4 conditions exhibit both laminar and turbulent flow and have thus been selected for a sample comparison with the reference-enthalpy method predictions in Figure 3. The agreement in the laminar region is reasonably good, but in the turbulent region the reference-enthalpy predictions are considerably higher than the experimental results. The usefulness of the reference enthalpy method for correlation purposes has been explored by examining $\left(\tau / \frac{1}{2} \rho_* u_e^2\right) \left(\rho_e u_e x' / \mu_*\right)^{0.2}$ as a function of local Reynolds number in Figure 4 for all of the sharp plate data. This approach is seen to correlate the turbulent data, but the average level of the reference-enthalpy data correlation falls quite far below the incompressible value of 0.0592. The skin friction measurements on the blunt plate (2-inch diameter leading edge) have been similarly correlated and are presented in Figure 5. The measured pressure distributions were used to compute local conditions based on an isentropic, equilibrium expansion from the leading edge stagnation point. The data once again correlate in terms of the reference-enthalpy parameters, but the average level of the correlation is further below the incompressible value than for the sharp plate case.

A more recent and promising approach to prediction of compressible turbulent flow is the calculation procedure developed by Spalding and Chi (Ref. 7), which postulates that a unique relation exists between $F_c C_f$ and $F_{R_x} Re_{e_x}$ or $F_{R_\theta} Re_{e_\theta}$ such that for a compressible turbulent flow, functions of Mach number and temperature ratio alone, viz., F_c, F_{R_x}, and F_{R_θ} may be found which relate the compressible flow identically to the incompressible one. Lacking sufficient experimental data, Spalding and Chi noted the comparative reliability of the theories based on mixing length and concluded that the function F_c could be evaluated from

$$F_c = \left[\int_0^1 \left(\frac{\rho}{\rho_e}\right)^{1/2} d\frac{u}{u_e}\right]^{-2} \tag{4}$$

Using a modified Crocco relation,

$$\frac{H_{eff} - H_w}{H_{AW} - H_w} = \frac{u}{u_e} \tag{5}$$

where

$$H_{eff} = h + r\frac{1}{2}u^2 \;,\quad H_{AW} = h_e + r\frac{1}{2}u_e^2 \;,\quad r = Pr^{1/3}$$

the static enthalpy is obtained as

$$\frac{h}{h_e} = \frac{H_w}{h_e} + \left(\frac{H_{AW}}{h_e} - \frac{h_w}{h_e}\right)\frac{u}{u_e} - \left(\frac{H_{AW}}{h_e} - 1\right)\left(\frac{u}{u_e}\right)^2 \tag{6}$$

from which follows the static temperature and the density needed in Eq. (4). Spalding and Chi obtained for F_{R_θ}

$$F_{R_\theta} = \left(\frac{T_{AW}}{T_w}\right)^{0.772} \Big/ \left(\frac{T_w}{T_e}\right)^{0.702} \tag{7}$$

based on fits of available heat transfer data, and also show that $F_{R_x} = F_{R_\theta}/F_c$. Because of the high adiabatic wall temperatures in the present application, it has been assumed that the adiabatic wall enthalpy is a more appropriate parameter, so that Eq. (7) is generalized as

$$F_{R_\theta} = \left(\frac{H_{AW}}{H_w}\right)^{0.772} \Big/ \left(\frac{H_w}{h_e}\right)^{0.702}$$

The Spalding and Chi prediction is shown for the zero angle of attack, Mach number 7.4 case in Figure 3. Although slightly below the data, the prediction is considerably superior to that of the reference enthalpy method. The functions F_c and F_{R_x} have therefore been computed using local conditions for all the sharp and blunt plate experiments and have been used to obtain $F_c C_f$ vs. $F_{R_x} Re_{e_x}$. The results are presented in Figures 6 and 7 compared to the correlation of incompressible data developed by Spalding and Chi. The sharp plate data are seen to correlate using these functions and to fall slightly above the semi-empirical theory curve. The zero angle of attack data, representing the highest local Mach number conditions, have the greatest departure from the Spalding and Chi prediction. The blunt plate data shown in Figure 7 not only correlate using the Spalding and Chi parameters, but are in even better agreement with the Spalding and Chi prediction than the sharp plate data. It appears that the higher local Mach number conditions on the sharp flat plate and the associated thicker laminar sublayers (Ref. 18) have a more important influence on turbulent boundary layer characteristics than the strong axial pressure gradients on the blunt plate, where the local Mach numbers remain relatively low (below 4).

Nozzle Wall Results

In examining the nozzle wall data, the measured pitot profiles have been used to obtain an integrated momentum thickness for the characteristic Reynolds number. This approach is possible with the present data for those cases in which the boundary layer profiles were obtained at essentially the same station as the wall measurements. Lacking a direct measurement of the local total enthalpy in the boundary layer, the unit Prandtl number, zero pressure gradient, Crocco relation, $u/u_e = (H - H_w)/(H_e - H_w)$, has been assumed, where the subscript "e" denotes boundary layer edge conditions and H denotes total enthalpy. Modifications to the Crocco relation are inferred from the wall measurements in the following section; however, for purposes of computing experimental values of momentum thickness the influence of the modifications is small -- on the order of 15 percent or less.

Velocity and density profiles were computed from the pitot profiles and the assumed Crocco relation as follows: 1) a Mach number profile is obtained from the pitot pressure profile assuming static pressure constant through the boundary layer, 2) the velocity profile follows from the energy equation and the Crocco relation, 3) static enthalpy and density can then be calculated using the energy equation and equation of state, respectively. The necessary velocity and density profiles are thus available to compute the momentum thickness.

Using the computed velocity and density profiles, integrations have been performed to obtain the displacement thickness, δ_*, and the momentum defect thickness, θ, which are expressed for the axially symmetric nozzle case as

$$\frac{\delta_*}{\delta} - \frac{\delta}{2r_w}\left(\frac{\delta_*}{\delta}\right)^2 = \int_0^1 \left(1 - \frac{\rho u}{\rho_e u_e}\right)\left(1 - \frac{y}{r_w}\right) d\frac{y}{\delta} \quad (8)$$

$$\frac{\theta}{\delta} - \frac{\delta}{2r_w}\left(\frac{\theta}{\delta}\right)^2 = \int_0^1 \frac{\rho u}{\rho_e u_e}\left(1 - \frac{u}{u_e}\right)\left(1 - \frac{y}{r_w}\right) d\frac{y}{\delta} \quad (9)$$

where r_w is the radius of the nozzle. These expressions collapse to the familiar two-dimensional forms when $\delta << r_w$. In the present cases the difference between the axially symmetric and the two-dimensional values was at most, ten percent.

The results for displacement thickness and momentum thickness are shown in Figure 8 compared with other experimental results as a function of Mach number. Measured pitot profiles and an assumed Crocco relation were used in the present case as well as in the results reported by Burke (Ref. 19) and in those obtained in a conical expansion nozzle at high stagnation temperatures. Measurements of both pitot pressure and total temperatures were

used by Lobb et al. (Ref. 20) and Hill (Ref. 21). The correlation of these results from the several sources indicates that the integrated displacement and momentum thicknesses are relatively insensitive to the assumption of the Crocco relation to pressure gradients and to high total temperatures. The present momentum thickness results are thus established for use in predictions for skin friction.

The experimental skin friction results are compared in Figure 9 with several predictions based on momentum thickness:

1. Blasius, reference enthalpy (Ref. 17) - The substitution of Eq. (3) in Eq. (2) yields the momentum thickness form for the Blasius, reference enthalpy shear law

$$\frac{\tau}{\frac{1}{2}\rho_* u_e^2} = 0.026 \left(\frac{\rho_e u_e \theta}{\mu_*} \right)^{-0.25} \tag{10}$$

An alternative to the Eckert reference enthalpy is obtained by using Eq. (6) in

$$h_{*_{Mean}} \equiv \int_0^1 h \, d\frac{u}{u_e} = 0.5 H_w + 0.333 h_e + 0.1667 H_{AW} \tag{11}$$

Although more general than the empirical Eckert reference enthalpy, the close similarity of the two approaches is evident upon comparison of Eqs. (1) and (11).

2. Spence, reference enthalpy (Ref. 22) - The shear law proposed by Spence on the basis of comparison with experimental results is

$$\frac{\tau}{\frac{1}{2}\rho_* u_e^2} = 0.0176 \left(\frac{\rho_e u_e \theta}{\mu_*} \right)^{-0.2} \tag{12}$$

3. Walz (Ref. 13) - The theory of Walz is computed using both his theoretical expressions for profile integral parameters and the experimentally determined ones.

4. Spalding and Chi (Ref. 7) - The factors F_c and F_{R_θ} required in the Spalding and Chi prediction are computed using Eqs. (4) and (7), respectively.

5. Winkler and Cha (Ref. 23) - A purely empirical evaluation of temperature ratio effects in compressible boundary layers with heat transfer resulted in the correlation formula

$$\left(\frac{T_o}{T_e}\right)^{1/2}\left(\frac{T_{AW}}{T_w}\right)^{1/4} C_f = 0.0246\left(Re_{e_\theta}\right)^{-0.257}$$

A comparison of each of the above with the normalized skin friction data at the last wall station is shown in Figure 9. The Walz (experimental profiles) approach considerably overpredicts the skin friction, whereas the Winkler-Cha correlation formula and the theoretical Walz expression fall far below the present data. The reference enthalpy method yields predictions slightly above the data. The most consistent agreement is provided by the semiempirical theory of Spalding and Chi, despite the fact that the experimental data on skin friction on which Spalding and Chi based their correlation factors were for low Mach number flows and, primarily, at near adiabatic wall conditions. The flow length Reynolds numbers for the nozzle data were also used to compare the experimental results with the Spalding and Chi prediction in Figure 10, where excellent agreement is noted.

Experimental Evaluation of Reynolds Analogy

Since both skin friction and heat transfer were measured in the experiments described, the relationship between skin friction coefficient and the Stanton number under cold wall, high Mach number conditions can be determined. Local flow conditions have been used both for the nozzle and the sharp flat plate experiments to compute the nondimensional coefficients, St_e and C_{f_e}, in the Reynolds analogy parameter, $2St_e / C_{f_e}$, which is presented for various values of the ratio of wall enthalpy to total enthalpy in Figure 11. The experimental results of Neal (Ref. 11) based on direct measurements of skin friction and heat transfer on a flat plate are also included. The results shown in Figure 11 indicate that the Reynolds analogy parameter $2St_e / C_{f_e}$ remains near or slightly above 1.0, except for the case with the lowest H_w / H_c. Whether this represents an

actual effect of extreme wall cooling remains for further investigation. These results indicate that the Stanton number is smaller with respect to skin friction coefficient than predicted by the modified Reynolds analogy of Colburn (Ref. 24), $2\,St_e / C_{f_e} = Pr^{-2/3}$, unless the Prandtl number is taken to be nearly unity (characteristic of turbulent Prandtl numbers) rather than evaluated at the laminar, wall value, which in the present case is approximately 0.72. The Reynolds analogy modifications of Rubesin (Ref. 25) and Monaghan (Ref. 5) are likewise too high. Bertram and Neal (Ref. 10) suggested that the Kármán theory for incompressible Reynolds analogy (Ref. 26) be applied to the compressible case by substituting an appropriate value of C_{f_i} in the Karman expression

$$2\,\frac{St_e}{C_{f_e}} = \left\{1 + 5\sqrt{\frac{C_{f_i}}{2}}\left[(Pr-1) + \log_e\left(\frac{5Pr+1}{6}\right)\right]\right\}^{-1} \qquad (13)$$

The experimental values of C_f in the present data have been related to an incompressible C_{f_i} using the Spalding and Chi theory. The result for $2\,St_e / C_{f_e}$ is in better agreement with the experimental data, but is still higher than the observed results.

Crocco Relation

The relationship between local velocity and total enthalpy in turbulent boundary layers has been investigated theoretically and experimentally by Cohen (Ref. 1), Spence (Ref. 22), Crocco (Ref. 3), Kutateladze and Leont'ev (Ref. 27), Walz (Ref. 13), and Rotta (Ref. 12), to name a few. The intent here is not to review these previous investigations, but is rather to identify the approximations implicit in the use of the Crocco relation and investigate the possibility of using the coupling between momentum and energy transfer to relate the experimental observations on the Reynolds analogy to modifications of the "Crocco relation" between velocity and total enthalpy. Using barred quantities to identify time averages and immediately assuming negligible pressure gradients normal to the wall, the turbulent boundary layer momentum and energy equations may be written (Ref. 27)

(energy and momentum)
$$\bar{\rho}\bar{u}\frac{\partial \bar{H}}{\partial x} + \bar{\rho}\bar{v}\frac{\partial \bar{H}}{\partial y} = \frac{\partial}{\partial y}\left\{\frac{\mu}{Pr}\frac{\partial \bar{H}}{\partial y} + \frac{k}{c_p}(Pr-1)\frac{\partial}{\partial y}\left(\bar{u}\frac{\partial \bar{u}}{\partial y}\right)\right\} \quad (14)$$

(momentum)
$$\bar{\rho}\bar{u}\frac{\partial u}{\partial x} + \bar{\rho}\bar{v}\frac{\partial \bar{u}}{\partial y} = \frac{\partial}{\partial y}\left(\mu\frac{\partial \bar{u}}{\partial y}\right) - \frac{dp}{dx} \quad (15)$$

It is clear that for the case $dp/dx = 0$ and $Pr = 1$, the last term in both equations vanishes and the differential equation for total enthalpy, $\bar{H}$, is identical with that for the velocity, $\bar{u}$. The boundary conditions $H = H_w$, $u = 0$ at $y = 0$ and $H = H_e$, $u = u_e$ at $y = \delta$ thus yield integrals of these equations which may be combined to yield the classical "Crocco relation"

$$\frac{H - H_w}{H_e - H_w} = \frac{u}{u_e} \quad (16)$$

Crocco (Ref. 3) and Cohen (Ref. 1) suggest a form

$$\frac{H - H_w}{H_e - H_w} = \left[1 - \left(\frac{c(x)}{1 - H_w/H_e}\right)\right]\frac{u}{u_e} + \frac{c(x)}{1 - H_w/H_e}\left(\frac{u}{u_e}\right)^2 \quad (17)$$

where the function $c(x)$ is intended to account approximately for the effects of Prandtl number and pressure gradients and yields the zero pressure gradient, unit Prandtl number form when $c(x) = 0$. The function $c(x)$ can be evaluated on the basis of wall measurements if it is assumed that $c(x)$ does not vary substantially across the boundary layer. The Reynolds analogy expression derived from

$$\frac{\dot{q}_w}{\tilde{c}_w} = \frac{\left(\frac{k}{c_p}\right)_w \left(\frac{\partial H}{\partial y}\right)_w}{\mu_w \left(\frac{\partial u}{\partial y}\right)_w}$$

yields

$$\frac{2C_H}{C_f} = \frac{1}{Pr_w}\left(1 - \frac{c}{1 - H_w/H_e}\right)$$

The Stanton number here is identified as C_H to indicate that it is based on total enthalpy rather than recovery enthalpy, $C_H = \dot{q}/(\rho_e u_e (H_e - H_w))$. The average values of the measured ratio of skin friction to heat transfer have been used to compute approximate values of c, assuming $Pr_w = 0.72$, with the following results:

Nozzle Test Condition	1	2	3	4	5	6	7
	0.27	0.28	0.31	0.28	0.28	0.30	0.28

Flat Plate Test Condition	1	2	3
	.26	.24	.18

These results indicate that the contoured nozzle and flat plate flows require comparable corrections to the Crocco relation, although the nozzle corrections are slightly larger. The small pressure gradient apparently had little effect on the nozzle wall boundary layer profiles. The values of C obtained from wall skin-friction and heat-transfer measurements have been used to compute total enthalpy profiles for comparison in Figure 12 with experimental measurements from several sources. (Figure 12 is a repeat of the data collection presented in Ref. 10 by Bertram and Neal.) The flat plate average value of $C = 0.228$ is seen to produce a profile in substantial agreement with the flat plate profile measurements. The value obtained from the present nozzle data ($C = 0.3$) agrees reasonably well with the profile measurements from nozzle wall experiments with the exception of the data reported by Hill (Ref. 21), which were obtained in a conical nozzle, having larger axial pressure gradients than in the other nozzle cases. It should be noted here that numerous investigators have observed good agreement between the Crocco relation ($C = 0$) and adiabatic wall experimental data. Baronti and Libby (Ref. 4), in applying the law of corresponding stations of Coles (Ref. 2) to a rigorous point-by-point mapping of the boundary layer profile, found that for boundary layer integrals and evaluation of the static temperature in the boundary layer, the unit Prandtl number form of the Crocco relation is satisfactory for all but Hill's conical nozzle data, where it was necessary to use the experimentally determined temperatures. The above results indicate that either pressure gradient effects or erroneous measurements caused this discrepancy rather than effects attributable to wall heat transfer or high Mach numbers.

Because the right hand side of the modified energy equation, Eq. (14), may be written

$$\left\{ \frac{\partial}{\partial y} \left[\bar{h} + Pr \frac{\bar{u}^2}{2} \right] \right\}$$

another effort to relax the restrictions in the Crocco relation has been to substitute for the total enthalpy an effective total enthalpy as in Eq. (5). This relationship is implicit in the Spalding and Chi evaluation of the skin friction coefficient correction factor, F_c , and has, in fact, been used by many other investigators including Walz (Ref. 13) and Rotta (Ref. 12) in their boundary layer profile studies. Equation (5) can also be written

$$\frac{H - H_w}{H_e - H_w} = \left[1 - \frac{\frac{(1-r)u_e^2}{2H_e}}{1 - H_w/H_e} \right] \frac{u}{u_e} + \frac{\frac{(1-r)u_e^2}{2H_e}}{1 - H_w/H_e} \left(\frac{u}{u_e} \right)^2 \qquad (18)$$

A comparison of Eqs. (17) and (18) reveals that this effective total enthalpy assumption implies a value of

$$C(x) = (1-r) \frac{u_e^2}{2H_e}$$

which, for the present experiments, lies in the range 0.095 to 0.1, if the recovery factor is taken as $Pr^{1/3}$ and the Prandtl number is taken as 0.72. This result for the relationship between total enthalpy and velocity is shown in Figure 12, where agreement with the outer portion of the measured flat plate profile is noted. The assumption of Eq. (18) implicit in the Spalding and Chi formulation appears to be justifiable and lends further support to the agreement noted between the Spalding and Chi theory and the experimental results on both the flat plates and the nozzle wall.

SUMMARY AND CONCLUSIONS

Using direct measurements of skin friction on sharp and blunt-leading-edge flat plates and on a contoured nozzle wall, the shear law for hypersonic, highly cooled turbulent boundary layers has been investigated. For the sharp plate the reference enthalpy extension of the classical, incompressible Blasius shear law is found to overpredict the skin friction, while the Spalding and Chi semiempirical theory is found to slightly underpredict the skin friction under these conditions. The blunt plate skin friction is smaller than predicted by the reference enthalpy extension, but is in excellent agreement with the theory of Spalding and Chi, despite the fact that the theory is derived for zero-pressure-gradient flows. Skin friction measured on a contoured nozzle wall is also found to agree with the Spalding and Chi theory as a function of Reynolds number based on both momentum thickness and flow length.

The experimental values of the Reynolds analogy parameter, from both the flat plate and nozzle measurements, are found to agree and to be slightly smaller than predicted by available theories. Corrections to the Crocco relation between total enthalpy and velocity in a turbulent boundary layer are inferred from the wall skin friction and heat transfer measurements from both the flat plate and the shock tunnel nozzle experiments. The resulting enthalpy-to-velocity relationship is shown to be consistent with direct measurements of boundary layer temperature profiles obtained by other investigators in flat plate and contoured nozzle experiments.

The close correspondence of the flat plate and contoured nozzle results for skin friction and for the Reynolds analogy parameter suggests that the boundary layers are basically similar. Further experimentation with detailed boundary layer profile measurements is required to develop a clearer picture, but a tentative conclusion is that turbulent boundary layers typical of flat plate flows can be developed on a contoured nozzle wall.

ACKNOWLEDGEMENTS

The flat plate experiments described herein were conducted under the sponsorship of the Air Force Flight Dynamics Laboratory, Contract No. AF 33(615)-1847, under the technical cognizance of Mr. V. Dahlem and Mr. M. Hillsamer (FDMG). The nozzle wall experiments described herein were conducted partially under the sponsorship of the NASA Office of Grants and Research Contracts, Contract No. NSR 33-009-029, and partially under the internal support of Cornell Aeronautical Laboratory. The NASA-supported work is under the technical cognizance of Mr. F. DeMeritte of NASA Headquarters and of Mr. I. Beckwith of the NASA Langley Research Center.

The author is especially indebted to Mr. A. Burke for his criticisms and suggestions in the final stages of this work.

NOMENCLATURE

c	Correction factor in Crocco relation
C_f	Local skin friction coefficient,
C_H	Stanton number, $\dot{q} / \rho u (H_o - H_w)$
d	Leading edge diameter
$F_{R\theta}$	Spalding and Chi Factor, $F_{R\theta} Re_\theta = Re_{\theta_i}$
F_c	Spalding and Chi factor, $F_c C_f = C_{f_i}$
F_{R_x}	Spalding and Chi factor, $F_{R_x} Re_x = Re_{x_i}$
h	Static enthalpy
H	Total enthalpy
k	Thermal conductivity
M	Mach number,
p	Static pressure
p_o	Reservoir pressure
p_s, p_o'	Stagnation pressure behind a normal shock
Pr	Prandtl number
q	Dynamic pressure,
$\dot{q}$	Heat transfer rate
r	Radial coordinate in nozzle, recovery factor
r_o	Leading edge radius
Re_x	Reynolds number based on distance x, $\frac{\rho u x}{\mu}$
s	Surface distance from geometric stagnation line
St	Stanton number
T	Temperature
u	Velocity
x	Axial distance from leading edge

y	Coordinate normal to flat plate surface
α	Angle of attack
δ	Boundary layer thickness
δ_*	Boundary layer displacement thickness
θ	Boundary layer momentum thickness
μ	Viscosity coefficient
ν	Kinematic viscosity,
ρ	Density
τ	Skin friction (shear stress at the wall)

Subscripts

o	Tunnel or free-stream stagnation conditions
AW	Adiabatic wall condition
e	Edge of the boundary layer, local flow conditions
i	Incompressible, constant density
r	Recovery
s	Stagnation point
w	Wall
$*$	Evaluated at reference temperature or enthalpy
∞	Free-stream condition

REFERENCES

1. Cohen, N. B., "A Method for Computing Turbulent Heat Transfer in the Presence of a Streamwise Pressure Gradient for Bodies in High-Speed Flow," NASA Memo 1-2-59L, March 1959.

2. Coles, D. E., "The Turbulent Boundary Layer in a Compressible Fluid," RAND Corp. Report R-403-PR, September 1962.

3. Crocco, L., "Transformation of the Compressible Turbulent Boundary Layer with Heat Exchange," AIAA, J. 1963, 2723-2731.

4. Baronti, P. O., and Libby, P. A., "Velocity Profiles in Turbulent Compressible Bounday Layers," AIAA, J., February 1966 (2), 193-202.

5. Monaghan, R. J., On the Behavior of Boundary Layers at Supersonic Speeds, in Flight International Aeronautical Conference, Los Angeles, New York: Institute of the Aeronautical Sciences, Inc., 1955.

6. Eckert, E. R. G., Engineering Relations for Friction and Heat Transfer to Surfaces in High Velocity Flow, J. Aeronautical Sciences, August 1956, 23, (8), 585-587.

7. Spalding, D. B. and Chi, S. W., The Drag of a Compressible Turbulent Boundary Layer on a Smooth Flat Plate with and Without Heat Transfer J. of Fluid Mechanics, January 1964, 18, (Part I), 117-143.

8. Bartz, D. R., Turbulent Boundary Layer Heat Transfer from Rapidly Accelerating Flow of Rocket Combustion Gases and of Heated Air, in Advances in Heat Transfer, Vol. 2, J. P. Harnett and T. F. Irvine, Jr. eds., New York: Academic Press, 1965.

9. Wood, N. B., "Calculation of the Turbulent Boundary Layer in the Nozzle of an Intermittent Axisymmetric Hypersonic Wind Tunnel," Aeronautical Research Council (G. B.), C. P. No. 721, September 1963.

10. Bertram, M. H. and Neal, L. Jr., "Recent Experiments in Hypersonic Turbulent Boundary Layers," NASA TMX-56335, May 1965.

11. Neal, Luther, Jr., "Pressure, Heat Transfer and Skin Friction Distributions over a Flat Plate having Various Degrees of Leading Edge Blunting at a Mach Number of 6.8," NASA TN D-3312, April 1966.

12. Rotta, J.C., Heat Transfer and Temperature Distribution in Turbulent Boundary Layers at Supersonic and Hypersonic Flow, in Recent Developments in Boundary Layer Research, AGARD ograph 97, Part I, Mary 1965, pp. 35-63.

13. Walz, A., "Compressible Turbulent Boundary Layers," The Mechanics of Turbulence, New York: Science Publishers, Inc., 1964 (Proceedings of Colloque Internationale sur "La Mechanique de la Turbulence," Marseille, August 28 to September 2, 1961).

14. MacArthur, R.C., "Transducer for Direct Measurement of Skin Friction in the Hypersonic Shock Tunnel," Cornell Aeronautical Laboratory, Inc., Report No. 129, August 1963 (AD 420-984).

15. Skinner, G., Analog Network to Convert Surface Temperature to Heat Flux, American Rocket Soc. J., 1960, 30, (6).

16. Wallace, J.E. and McLaughlin, E.J., "Experimental Investigations o of Hypersonic, Turbulent Flow and Laminar, Leeward-Side Flow on Flat Plates," AFFDL-TR-66-63, Vol. I, July 1966.

17. Lin, C.C., Turbulent Flows and Heat Transfer, Vol. V, High Speed Aerodynamics and Jet Propulsion, Princeton, N.J.: Princeton University Press, 1959.

18. Donaldson, C. duP., "Heat Transfer and Skin Friction for Turbulent Boundary Layers on Heated or Cooled Surfaces at High Speeds," NACA RML52H04, October 1952.

19. Burke, A.F., "Turbulent Boundary Layers on Highly Cooled Surfaces at High Mach Numbers," Cornell Aeronautical Laboratory, Inc., Report No. 118, November 1961.

20. Lobb, R.K., Winkler, E.M., and Persh, S., Experimental Investigation of Turbulent Boundary Layers in Hypersonic Flows, J. Aeronautical Sciences, 22, (1), January 1955, 1-8 (Also as NAVORD Report 3880, 1955).

21. Hill, F.K., "Turbulent Boundary Layer Measurements at Mach Numbers of 8 to 10," Physics of Fluids, 1959, 2, 668-680.

22. Spence, D.A., "Some Applications of Crocco's Integral for the Turbulent Boundary Layer," Proceedings of the 1960 Heat Transfer and Fluid Mechanics Institute, Stanford University Press, California, 1960.

23. Winkler, E.M. and Cha, M., "Investigation of Flat Plate Hypersonic Turbulent Boundary Layer with Heat Transfer at a Mach Number of 5.2," NAVORD Report 6631, 1959.

24. Colburn, A.P., A Method of Correlating Forced Convection Heat Transfer and a Comparison with Fluid Friction, Trans. of the American Institute of Chemical Engineers, 1933, 29, 174-210.

25. Rubesin, M.W., "A Modified Reynolds Analogy for the Compressible Turbulent Boundary Layer on a Flat Plate," NACA TN 2917, March 1953.

26. von Karman, Th. The Analogy Between Fluid Friction and Heat Transfer, ASME Trans., November 1939, 61, (8), 705-710

27. Kutateladze, S.S. and Leont'ev, A.I. (Translated by D.B. Spalding) Turbulent Boundary Layers in Compressible Gases, New York: Academic Press, 1964.

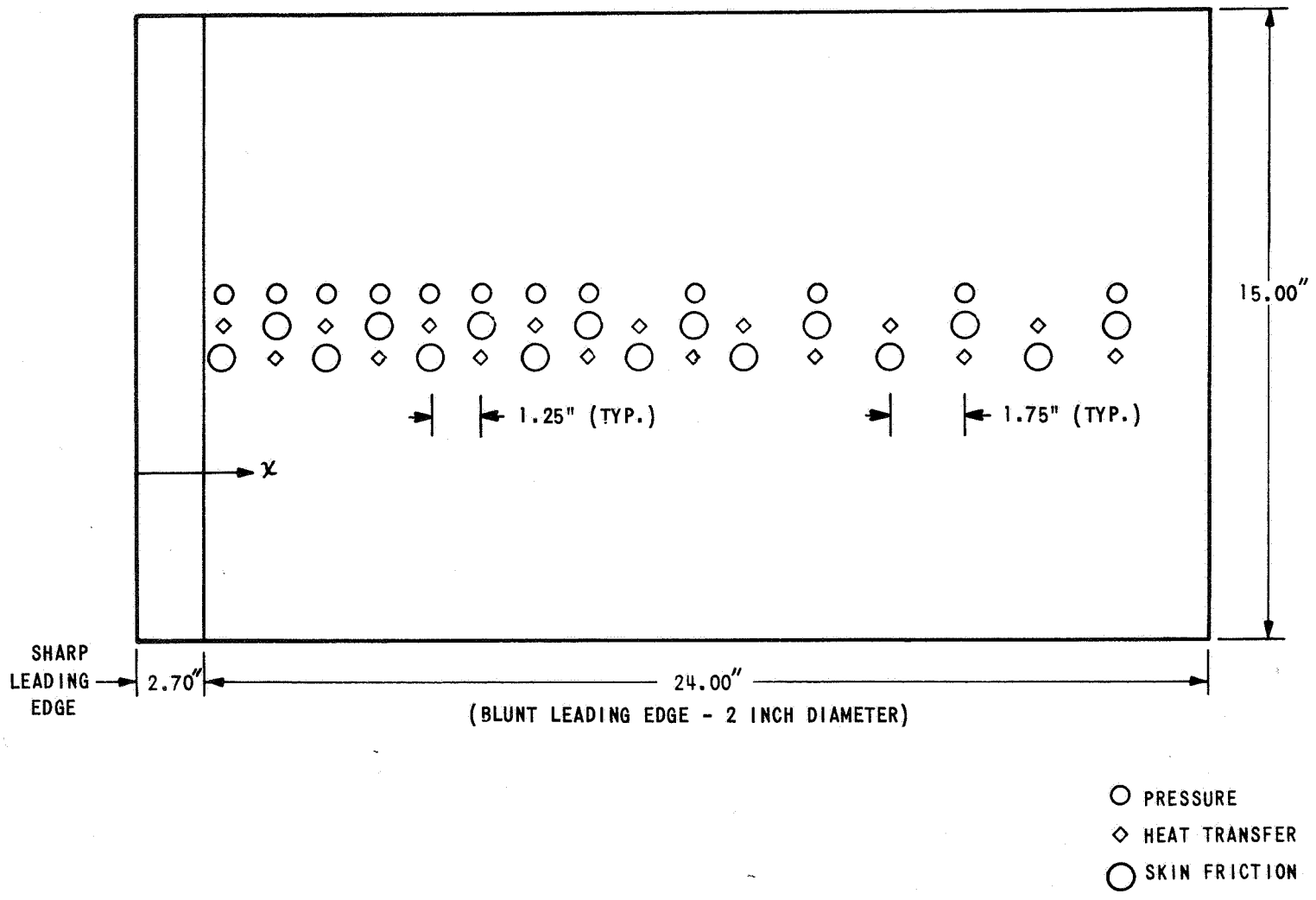


Figure 1 FLAT PLATE MODEL INSTRUMENTATION

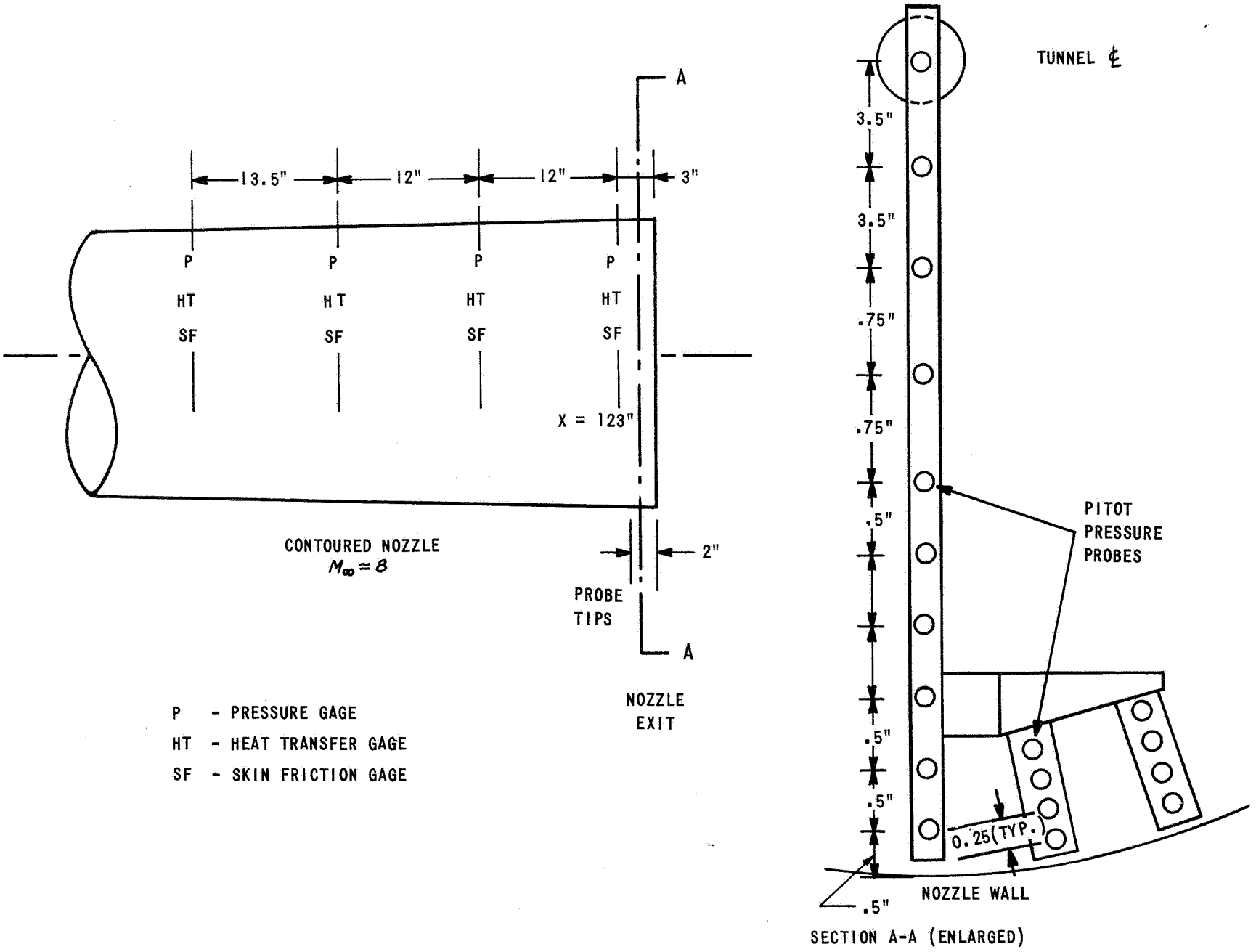


Figure 2 NOZZLE BOUNDARY LAYER INSTRUMENTATION

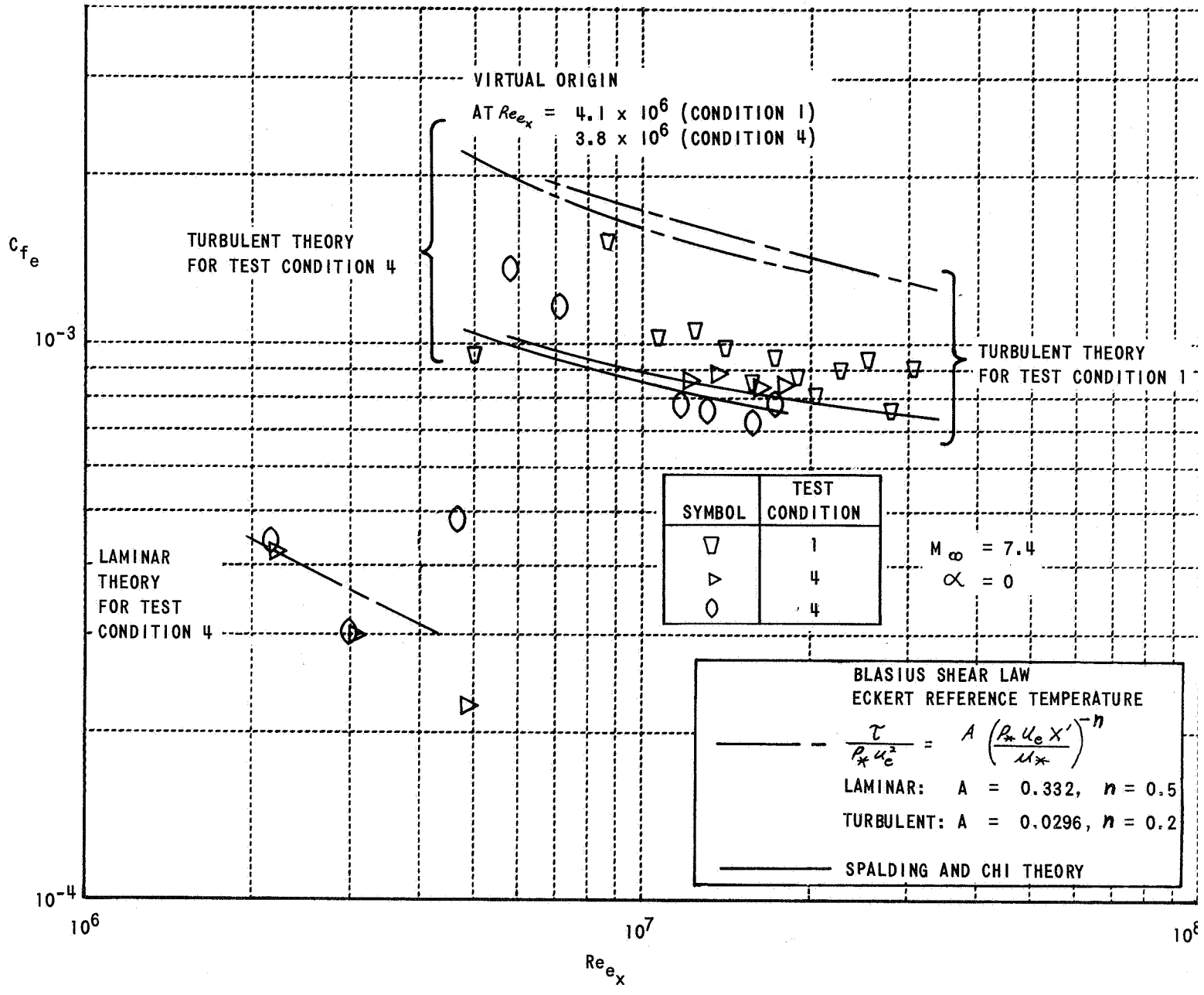


Figure 3 COMPARISON OF SHARP FLAT PLATE SKIN FRICTION WITH TURBULENT FLOW THEORY

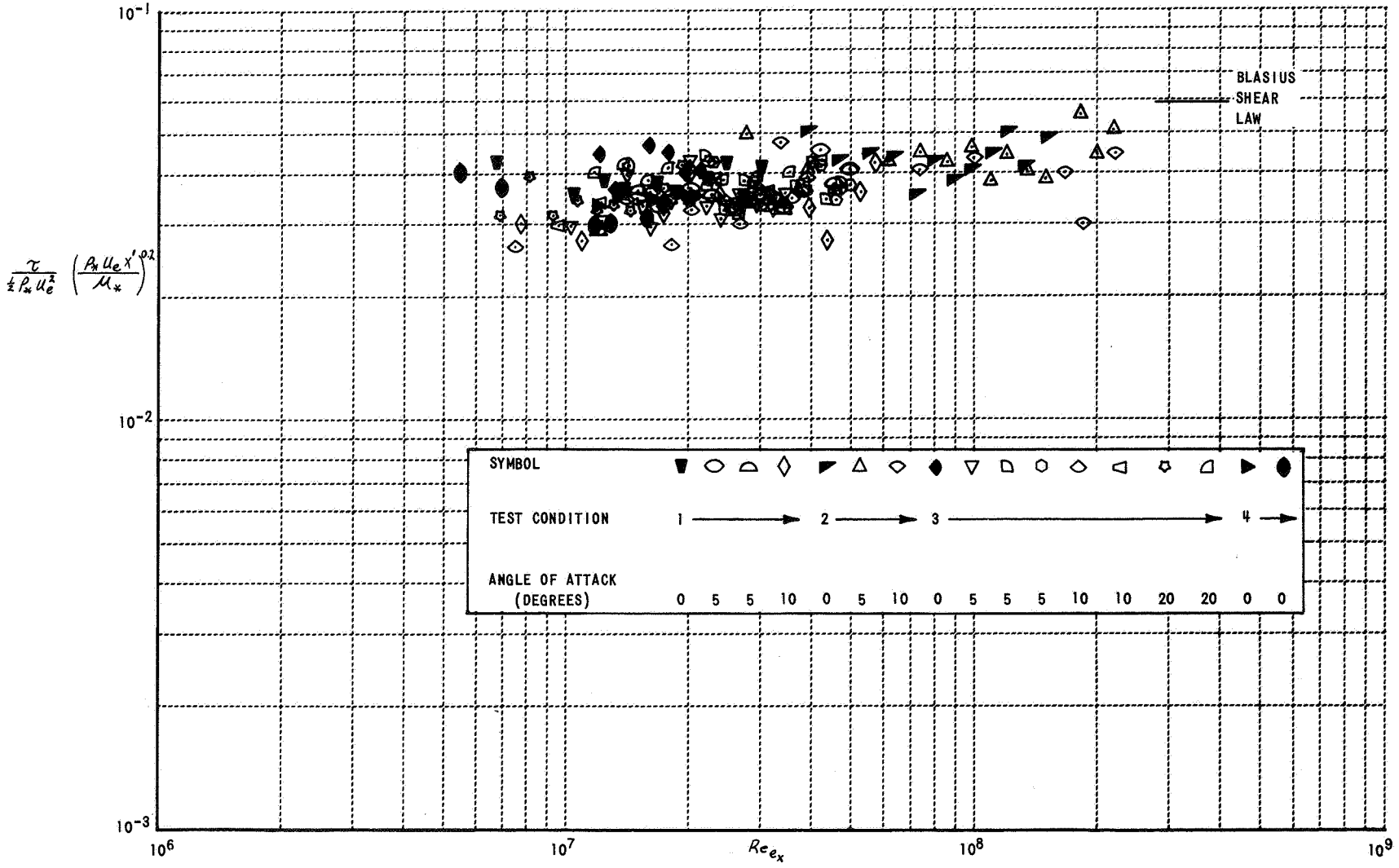


Figure 4 SHARP FLAT PLATE SKIN FRICTION CORRELATION USING ECKERT REFERENCE ENTHALPY

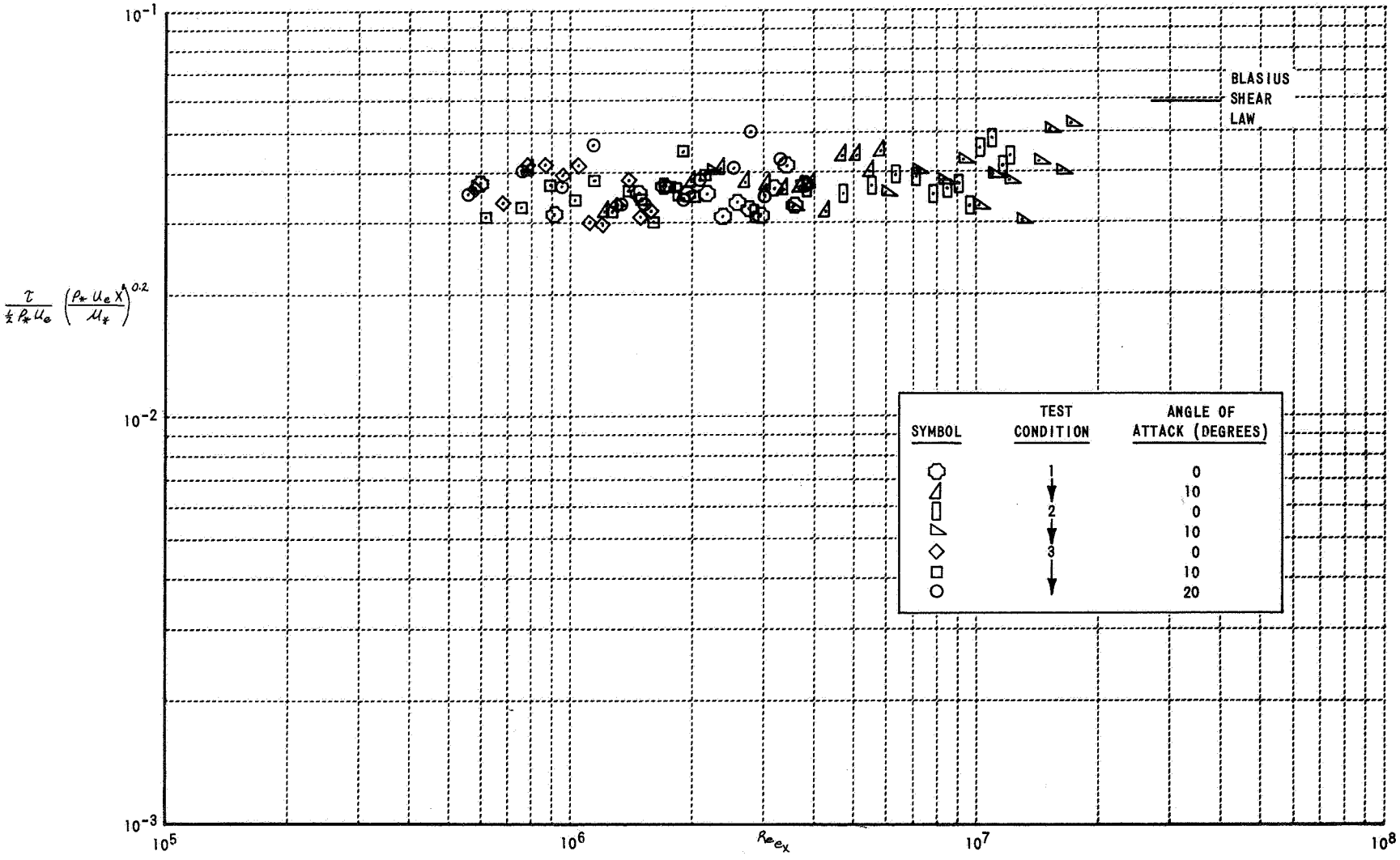


Figure 5 BLUNT FLAT PLATE SKIN FRICTION CORRELATION USING ECKERT REFERENCE ENTHALPY

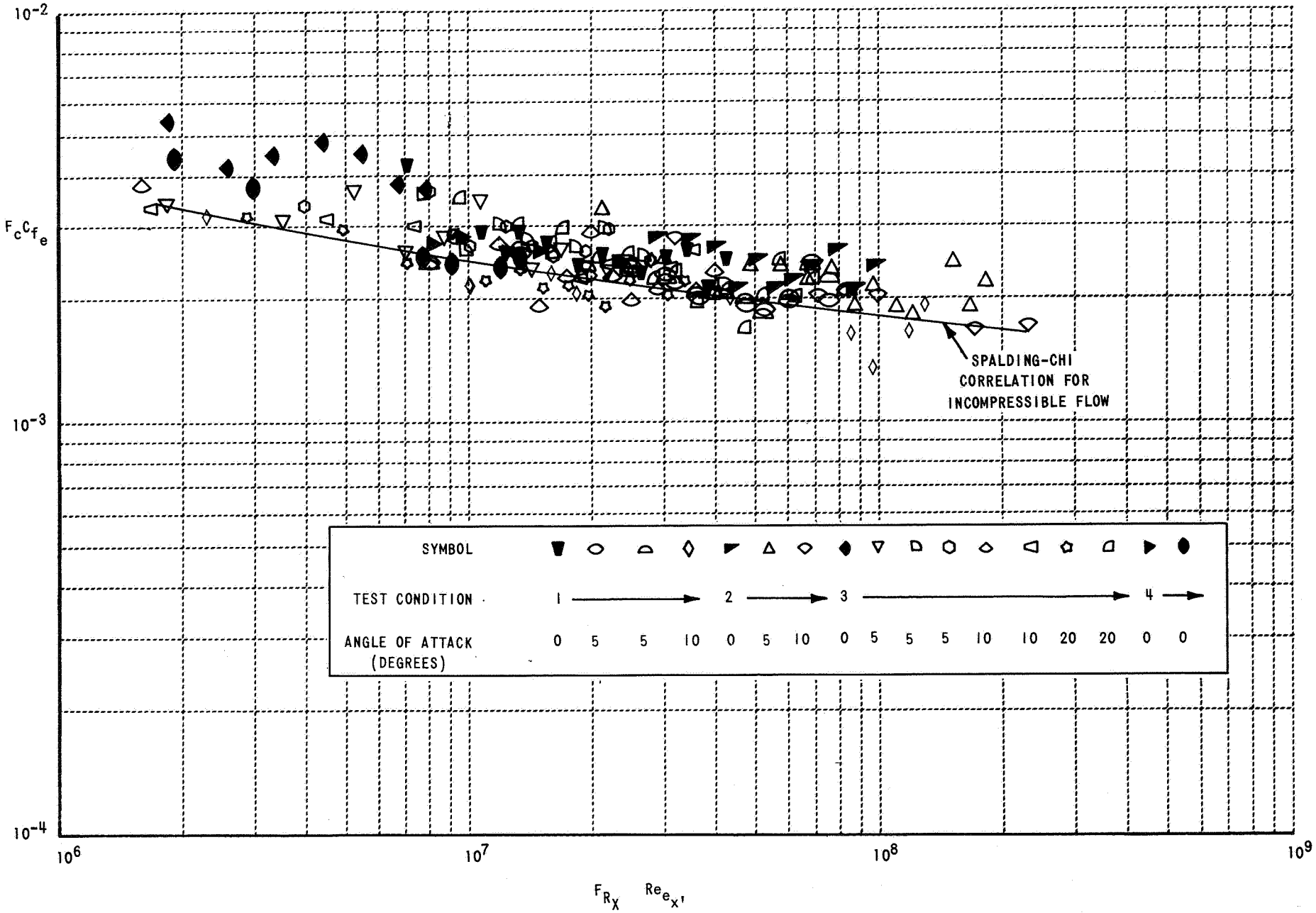


Figure 6 SHARP FLAT PLATE SKIN FRICTION CORRELATION WITH SPALDING-CHI THEORY

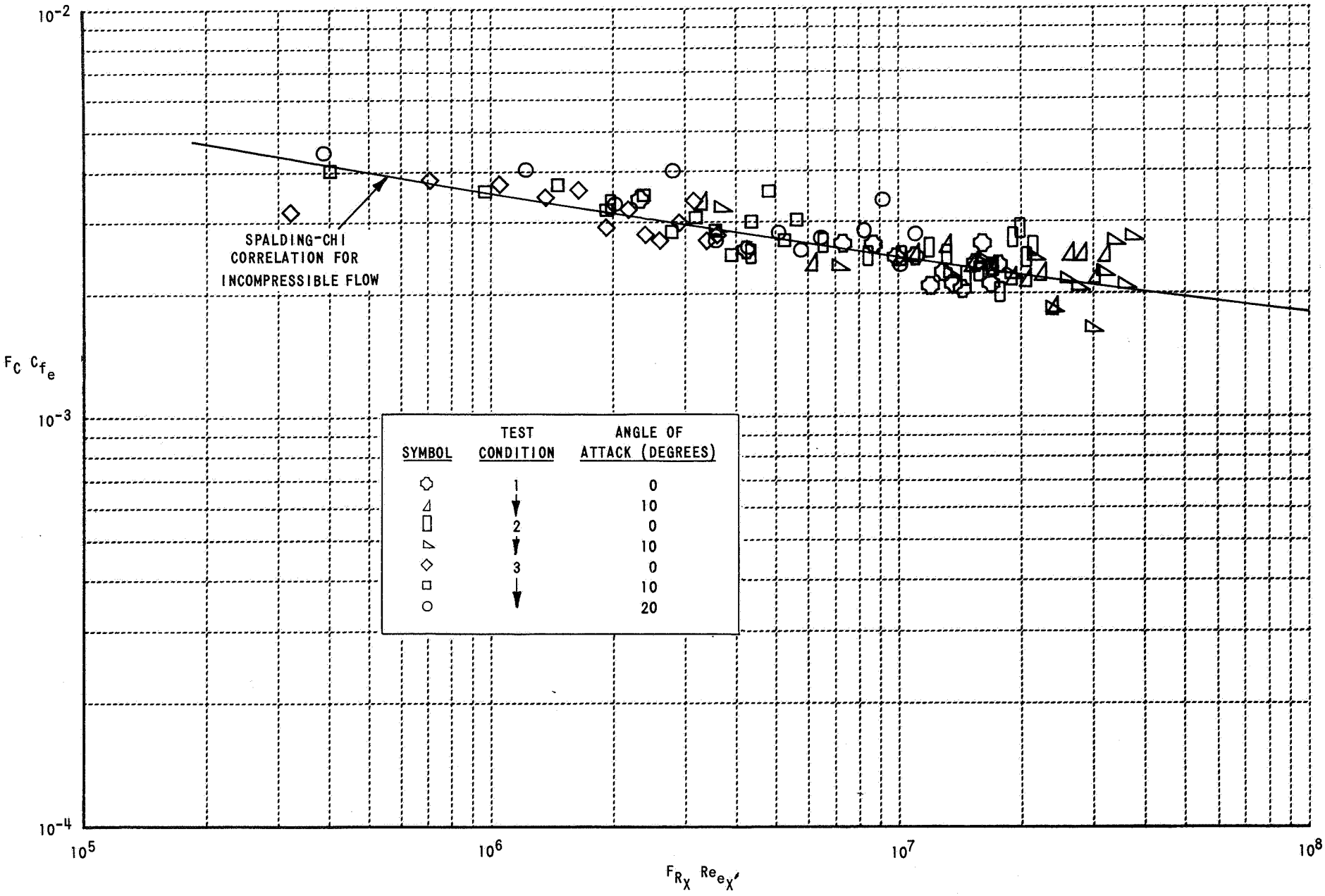


Figure 7 BLUNT FLAT PLATE SKIN FRICTION CORRELATION WITH SPALDING - CHI THEORY

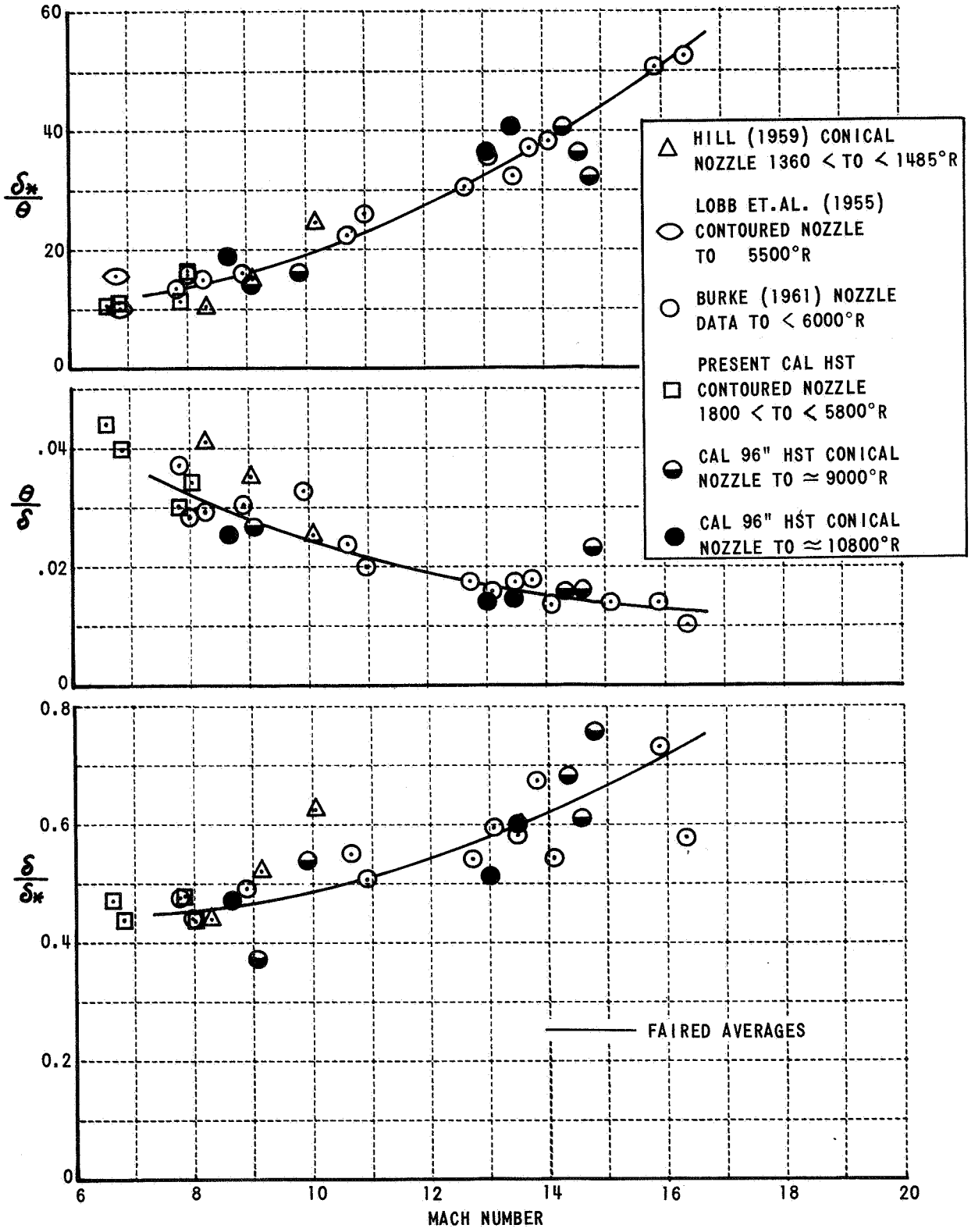


Figure 8 TURBULENT BOUNDARY LAYER DISPLACEMENT AND MOMENTUM THICKNESSES FROM SHOCK TUNNEL NOZZLE DATA

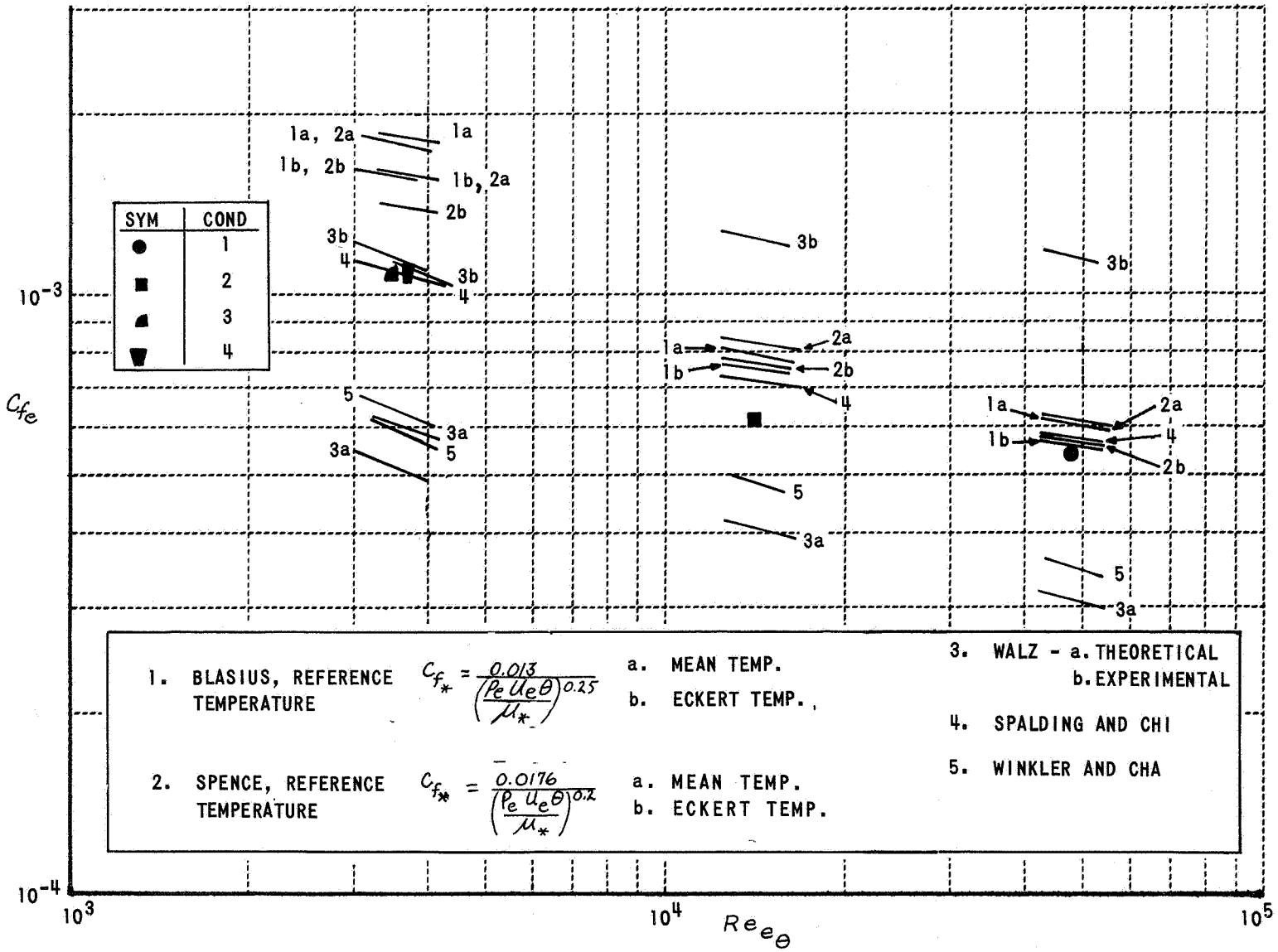


Figure 9 NOZZLE WALL SKIN FRICTION COEFFICIENT VS. MOMENTUM THICKNESS REYNOLDS NUMBER

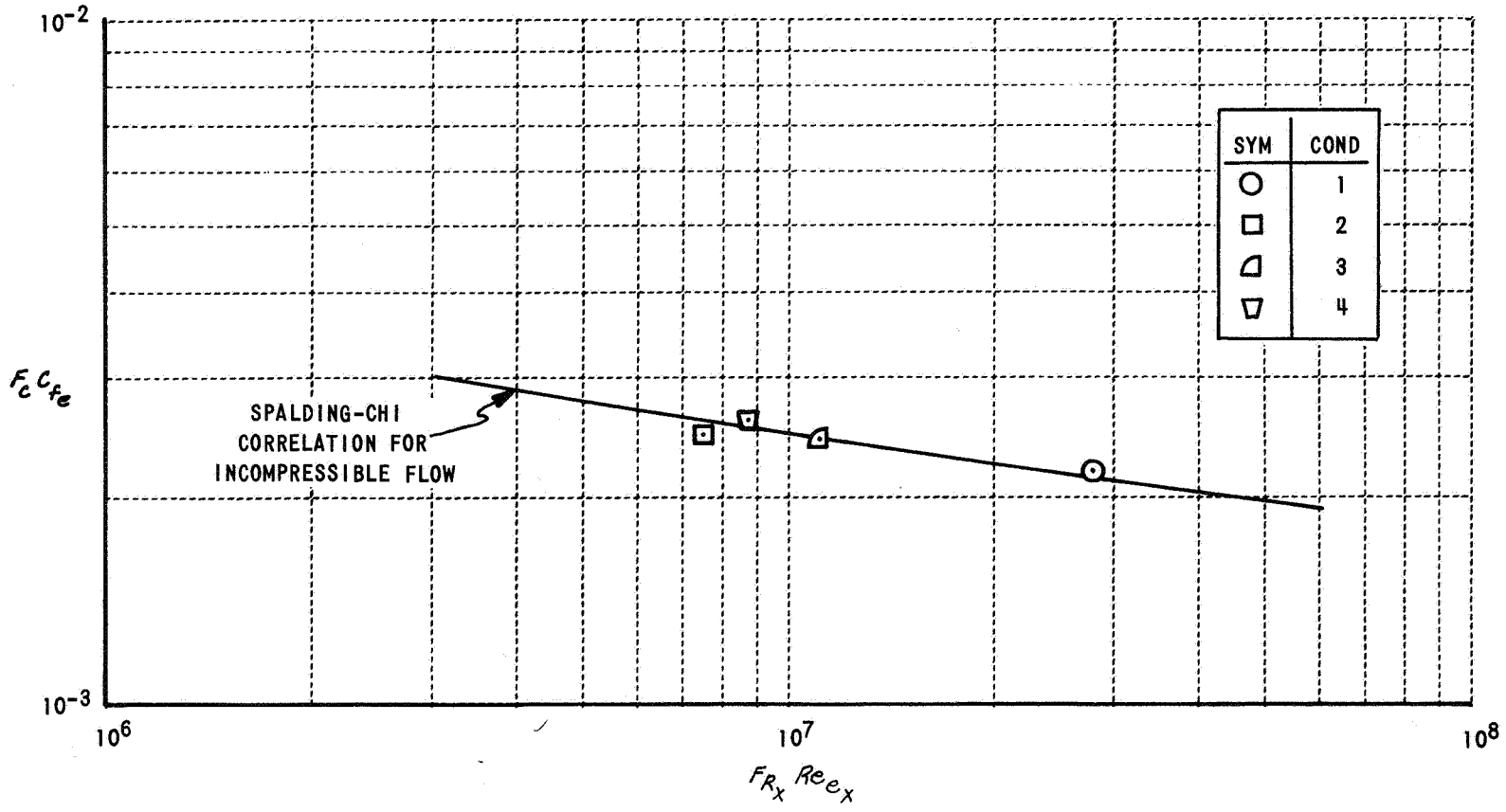


Figure 10 SPALDING-CHI CORRELATION OF NOZZLE WALL SKIN FRICTION

SOURCE	SYM	M_e	$Re\left(\frac{\times 10^6}{ft}\right)$	T_o (°R)
NASA TN D-3212, FLAT PLATE	■	6.8	4.5 TO 8.0	1100
FLAT PLATE - CAL 8′ SHOCK TUNNEL	●	10.7	15.	2800
	▲	8.1	81	1800
● α = 0° ◐ 10° ◔ 20°	⬬	7.4	20	3800
INSTRUMENTED NOZZLE WALL CAL 4′ AND 8′ SHOCK TUNNELS	○	8.0	11	1850
	□	7.8	2.6	1800
	◁	6.6	.37	5750
	▽	6.8	.44	5000
	◇	7.8	4.1	2300
	◇	8.0	9.7	2400
	◇	7.6	1.0	2200

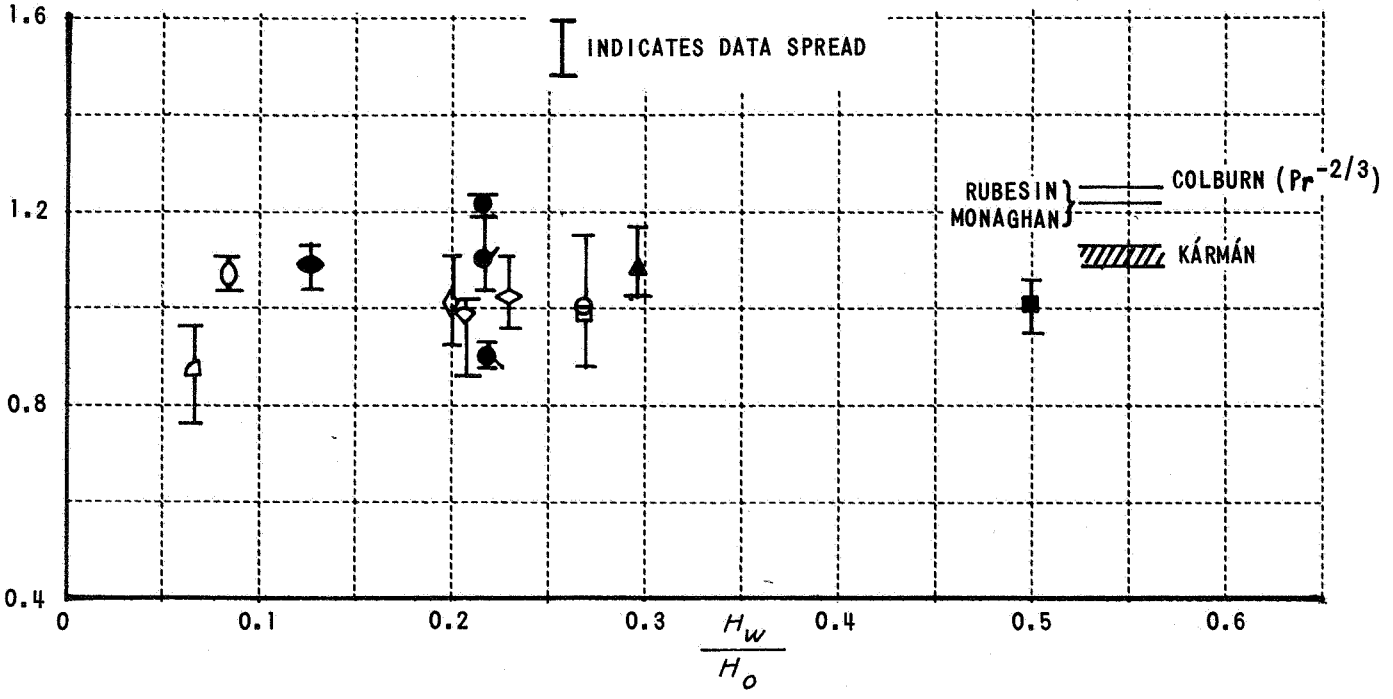


Figure 11 REYNOLDS ANALOGY FOR TURBULENT FLOWS WITH HEAT TRANSFER TO THE WALL

	M_e	$Re_e \times 10^{-4}$	T_o (°R)	MODEL	SOURCE
◆	6.4	.60	990	FLAT PLATE	DANBERG, NOL TR64-99
□	6.8	1.30	1110	NOZZLE TEST SECTION	BERTRAM AND NEAL, NASA TMX-56335
△	9.1	.19	1360	CONICAL NOZZLE	HILL , PHYS. FLUIDS, 1959
◺	5.1	.74	1012	WEDGE NOZZLE	LOBB, WINKLER, AND PERSH, NAVORD 3880
▽	6.8	1.26	1055		
◿	7.7	.81	1162		
▽	8.2	.95	1180		

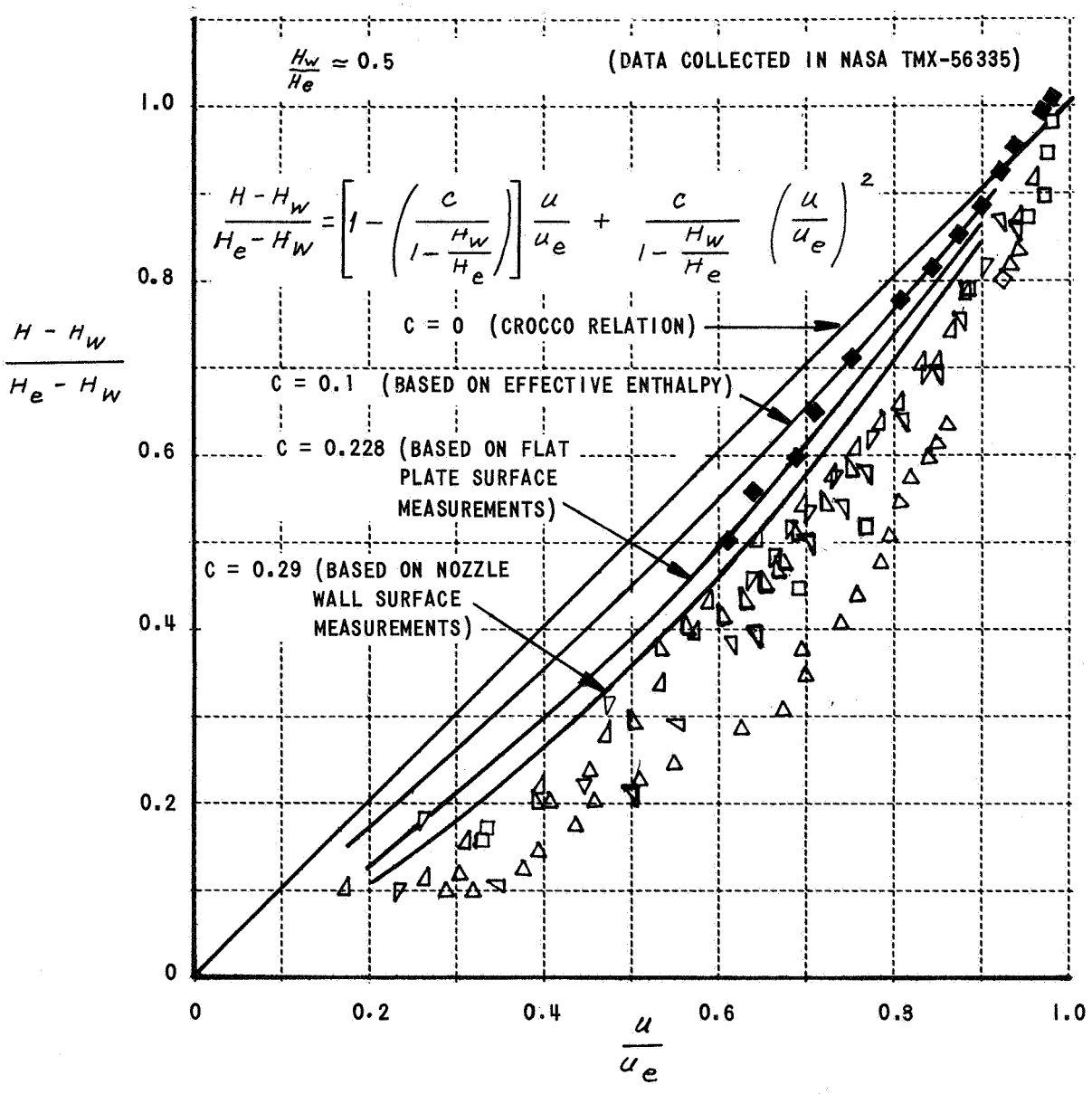


Figure 12 ENTHALPY - VELOCITY PROFILES IN A TURBULENT BOUNDARY LAYER